Close coupling calculations for rotational relaxation of CO in argon: Accuracy of energy corrected sudden scaling procedures and comparison with experimental data

R. Z. Martinez, J. L. Domenech, D. Bermejo, F. Thibault, J.-P. Bouanich et al.

Citation: J. Chem. Phys. **119**, 10563 (2003); doi: 10.1063/1.1620506
View online: http://dx.doi.org/10.1063/1.1620506
View Table of Contents: http://jcp.aip.org/resource/1/JCPSA6/v119/i20
Published by the AIP Publishing LLC.

Close coupling calculations for rotational relaxation of CO in argon: Accuracy of energy corrected sudden scaling procedures and comparison with experimental data

R. Z. Martinez, J. L. Domenech, and D. Bermejo
Instituto de Estructura de la Materia, C.S.I.C. Serrano 123, 28006 Madrid, Spain

F. Thibault[a)]
Laboratoire de Physique des Atomes Lasers Molécules et Surfaces (UMR-CNRS 6627), Université de Rennes I, Campus de Beaulieu, F-35042 Rennes Cedex, France

J.-P. Bouanich and C. Boulet
Laboratoire de Photophysique Moléculaire (CNRS), Université de Paris Sud Bât. 350, Campus d'Orsay, F-91405 Orsay Cedex, France

(Received 27 May 2003; accepted 29 August 2003)

Fully quantal scattering calculations are carried out for CO in argon using both the close coupling (CC) and coupled states (CS) methods. CC and CS cross sections $\sigma(j \rightarrow j')$ generally agree to within 15% or less with the exception of those corresponding to low $\Delta j = |j' - j|$ values at low j where differences may reach 50%. The discrepancy arises mostly from efficient collisions with large orbital angular momentum, where the rotation of the quantization axis can no longer be neglected. Then, the CC calculations were used to test a scaling procedure based on the energy corrected sudden (ECS) approximation: given a set of basic cross-section $\sigma(j \rightarrow 0)$, is it possible to predict the entire $\sigma^o(j \rightarrow j')$ relaxation matrix? The ECS procedure yields reasonable agreement, *on average*, at the 13% level. However it fails at reproducing the $\Delta j = 1$ cross sections in cases where the concept of a mean adiabaticity factor losses its physical meaning since the duration of the efficient collisions varies too much with the orbital angular momentum. On that basis, we have examined another question: the validity of an inversion procedure, based on the ECS scheme. Is it possible to determine the basic cross sections $\sigma(j \rightarrow 0)$ starting from the knowledge of the easily measurable diagonal elements $\sigma^o(j \rightarrow j)$? The ECS inverted basic rates agree with the CC ones to within about 20% up to $j = 15$ and strongly diverge for higher j while the inversion leads to an overestimation of the mean duration of the efficient collisions. Then, using a high resolution Raman spectrometer, we recorded the *Q*-branch head of the fundamental band of CO in mixture with Ar at three temperatures, 87, 195, and 300 K, and total pressures up to 1.25 bar. Line-mixing effects in experimental Raman profiles are compared with CC theoretical predictions. Finally the close coupling results are also used to predict rotational relaxation times measured in free jets. © *2003 American Institute of Physics.* [DOI: 10.1063/1.1620506]

I. INTRODUCTION

Rotational energy transfer influences many fundamental processes such as absorption in a gas, population evolution of nonequilibrium systems, optical pumping processes,[1] etc. Numerous experimental studies of gas-phase rotational relaxation are now available, but a main difficulty subsists in the analysis of these data: the very large number of state-to-state rate constants needed to describe relaxation phenomena due to the large number of rotational levels typically accessible.

Therefore, it is particularly interesting to develop efficient scaling laws to fit the whole rate constant matrix in terms of a few parameters.[2] Among the various available methods, the energy corrected sudden (ECS) approximation of DePristo *et al.*[3] is probably the most powerful one and has been widely used in various fields and for many molecular systems.[2,4,5]

Let us briefly recall the main features of the ECS scaling procedure. It allows one to write the entire matrix of rate constants, $\sigma(j \rightarrow j', T)$, in terms of a fundamental set described by the most convenient rate constants in the fundamental level $\sigma(j \rightarrow 0, T)$ and a critical duration of collisions $\overline{\tau_c}$ appearing in adiabaticity factors that takes into account inelastic energy changes, at least approximately. As a preliminary step, and extending a previous work of Green *et al.*,[6] we analyze in Sec. III the accuracy of the ECS approximation: how accurately does it predict the entire matrix of $\sigma(j \rightarrow j', T)$ rate constants considering that the fundamental rates $\sigma(j \rightarrow 0, T)$ are independently known?

On that basis, it will be possible, in a second step, to examine another question: the validity of inversion procedures based on the ECS frame. It is possible to determine the basic cross sections $\sigma(j \rightarrow 0, T)$ starting from the knowledge of the easily measurable diagonal elements (pressure broad-

a)Author to whom all correspondence should be addressed. Electronic mail: franck.thibault@univ-rennesl.fr

ening cross sections) $\sigma^o(j\rightarrow j,T)$? In this approach, the basic rates $\sigma(j\rightarrow 0,T)$ are modeled through various analytical forms [see Ref. 2 and Eq. (9) in Sec. IV], characterized by several fitting parameters. These parameters are varied along with the critical duration of collisions to fit extensive sets of experimental data. One of the objectives of this paper, presented in Sec. IV, is to carefully analyze the ability of this inversion procedure to model the basic rates and therefore the whole relaxation matrix.

The present work tests the accuracy of the ECS scaling law for CO–Ar collisions. In a recent paper,[7] a similar study has been done on CO–He collisions. However, collisions with helium are not a very stringent test since, due to the smaller reduced mass μ, they may be considered as sudden, leading to scaling laws rather insensitive to adiabaticity corrections and, then, to the critical duration. In a preliminary study,[8] both close coupling (CC) and coupled states (CS) calculations have been carried out for the diagonal elements of the CO–Ar relaxation matrix. They used the accurate intermolecular potential surface (IPS) of Tockzylowski and Cybulski[9] (TC potential in the following). CC-pressure broadening cross sections were found to be in good agreement with experimental data and some failings of the CS approximation were pointed out. In Sec. II, using the same potential we extend the analysis of the accuracy of the CS approximation to the nondiagonal elements. Finally, we analyze the ability of our benchmark CC calculations to interpret some recent measurements[10] of rotational relaxation times in free jets (Sec. VI) as well as line-mixing effects in isotropic Raman Q branch of CO in Ar (Sec. V). For that purpose, experimental profiles at three temperatures (87, 195, and 300 K) and pressures up to 1250 mbar have been recorded with the stimulated Raman spectrometer located in Madrid.

II. THEORY AND QUANTAL RESULTS

A. Theoretical framework and computational methods

First of all, let us note that, since the TC potential does not depend on the CO vibrational stretching coordinate, we will consider CO as a rigid rotor. Thus any vibrational effects are neglected. They are known to be very weak[8] except for IR line shifts[11] and we will omit in the following the vibrational quantum number subscripts on the cross sections.

The total angular momentum J-coupling scheme of the scattering of an atom by a rigid rotor as formulated by Arthurs and Dalgarno[12] is the starting point in the CC method. It has been reviewed in the CO–He work of Green *et al.*[13] and will not be detailed here. The CC expressions for the inelastic state-to-state cross sections are

$$\sigma_{\mathrm{CC}}(j\rightarrow j',E_{\mathrm{kin}}) = \sum_J (2J+1)\frac{\pi}{k^2}\frac{1}{2j+1}\sum_{\ell\ell'} |\langle j'\ell'|S^J(E_{\mathrm{kin}}+E_j|j\ell\rangle|^2 = \sum_J \sigma_{\mathrm{CC}}(j\rightarrow j',E_{\mathrm{kin}},J), \quad (1)$$

where $E_{\mathrm{kin}}=\hbar^2k^2/2\mu$ is the (initial) barycentric kinetic energy of a collision and ℓ and ℓ' are the orbital angular momenta before and after a collision, respectively. In the "ℓ-labeled" CS approximation,[14] $\ell=\ell'$ and there is an additional label, λ, which is the projection of j onto the intermolecular axis, leading to the formally identical expression

$$\sigma_{\mathrm{CS}}(j\rightarrow j',E_{\mathrm{kin}}) = \sum_\ell (2\ell+1)\frac{\pi}{k^2}\frac{1}{2j+1}\sum_\lambda |\langle j'|S^{\ell\lambda}(E_{\mathrm{kin}}+E_j|j\rangle|^2 = \sum_\ell \sigma_{\mathrm{CS}}(j\rightarrow j',E_{\mathrm{kin}},\ell). \quad (2)$$

The calculations of the state-to-state cross sections were performed for convenience with both MOLSCAT[15] and MOLCOL[16] codes. However, the CS approximation is only implemented in MOLSCAT code. Some details on the way of solving the coupled equations may be found in Ref. 8.

The kinetic energy dependent cross sections of Eqs. (1) and (2) must be thermally averaged over the Boltzmann distribution of kinetic energies to provide temperature dependent rotational rate constants, denoted as $\sigma(j\rightarrow j',T)$ in the following.

Finally, let us recall that the line coupling cross section $\sigma^o(j\rightarrow j')$ describing the coupling of two isotropic Raman $Q(j)$ and $Q(j')$ lines is just the inelastic state-to-state rate $\sigma(j\rightarrow j')$ with opposite sign. Due to the unitarity of the diffusion operator, these cross sections, either in the CC or CS scheme, satisfy the following sum rule, at least in the rigid rotor limit:

$$\sum_{j'\neq j}\sigma^o(j\rightarrow j',E_{\mathrm{kin}}) = -\sigma^o(j\rightarrow j,E_{\mathrm{kin}}), \quad (3)$$

where the diagonal element is the broadening cross section of the corresponding isotropic Raman $Q(j)$ line. Of course, it can be easily verified that the T-dependent cross sections also satisfy a similar sum rule. Furthermore, as is well known, they verify the detailed balance principle.[7,17]

B. Accuracy of the coupled states approximation

There are different levels of detail, ranging from fine to gross, at which the CC and CS results can be compared:[17] these are the rotational dependence at a fixed kinetic energy, the energy dependence, the temperature dependence, etc.

Let us begin by considering CC and CS calculations at a kinetic energy E_{kin} of 265 cm^{-1} corresponding approximately to the energy $(4/\pi)k_BT$ for the mean relative velocity at room temperature, which is the maximum of the relative velocity distribution. Some illustrative results are given in Tables I and II. A detailed analysis shows that CC and CS cross sections are rather similar to one another (within 10%–15%) with the exception of those corresponding to low Δj values (mainly $\Delta j=\pm 1$) at low j values ($0\leqslant j\leqslant 6$) where differences may reach 50%. Figure 1 illustrates the partial wave contributions to two cross sections. Such differences have already been reported by Launay[18] even for CO–He where the CS approximation is expected to be better than for CO–Ar. These discrepancies may be easily understood within a semiclassical picture through the analysis of the

TABLE I. Inelastic cross sections $\sigma(j \rightarrow j')$ (i.e., Raman isotropic line coupling cross sections with opposite sign) and pressure broadening cross sections for $j=j'$ (in Å^2) at $E_k=265$ cm^{-1} and for high j values. The first line corresponds to the CC results and the second line to the CS results.

j	$j'=0$	CS/CC	$j'=2$	CS/CC	$j'=8$	CS/CC	$j'=14$	CS/CC
8	0.214		1.122		53.36			
	0.248	1.159	1.155	1.03	52.54	0.985		
9	0.429		2.124		8.5		1.48	
	0.428	0.998	2.07	0.975	9.23	1.086	1.37	0.926
10	0.241		1.13		4.915		2.47	
	0.294	1.22	1.326	1.173	4.19	0.852	2.32	0.939
11	0.152		0.833		5.184		3.22	
	0.128	0.842	0.665	0.798	4.84	0.934	3.03	0.941
12	0.193		0.938		2.274		4.46	
	0.182	0.943	0.875	0.933	2.9	1.053	4.58	1.027
13	0.0904		0.459		2.47		10.14	
	0.0981	1.085	0.471	1.026	2.17	0.879	10.27	1.013
14	0.0922		0.476		2.15		50.78	
	0.0748	0.811	0.383	0.805	2.04	0.949	50.5	0.9945
15	0.0875		0.429		1.43		10.86	
	0.0843	0.963	0.405	0.944	1.41	0.986	11.17	1.0285

partial CC and CS cross sections versus $J(\ell)$ which are given in Fig. 1. For that purpose we consider the parabolic trajectory around the distance of closest approach r_c as introduced by Robert and Bonamy.[19] The classical impact parameter b may be related to ℓ (or J) through the usual relation $\hbar^2\ell(\ell+1)=2\mu E_{\text{kin}}b^2$. The duration of collision, defined by $\tau_c=r_c/v_c'$ (v_c' is an effective velocity near the distance of closest approach r_c) as a function of b for $E_{\text{kin}}=265$ cm^{-1} is plotted in Fig. 2, where it appears that collisions may be classified in two categories. Those corresponding to J (or ℓ) values lower than 70—which are primarily driven by the repulsive part of the potential—have quite the same duration, and are known as leading to classical deflections of the order of π. Consequently, the rotation of the quantization axis around the distance of closest approach may be reasonably neglected for these collisions. Those corresponding to J (or ℓ) >70, where the long-range attractive part becomes more important, have durations which strongly depend on b (J or ℓ) and involve very small classical deflections. Therefore, they involve a significant rotation of the quantization axis. For low j and low $|\Delta j|$ values, partial waves higher than 70 are predominant [cf. Fig. 1(a)] and the CC and CS cross sections may be very different. We are in a situation rather similar to that analyzed by Roche *et al.*[20] in the CO_2–Ar case within a perturbative semiclassical formulation. By contrast, for high j or high $|\Delta j|$ values [Fig. 1(b)], low partial waves corresponding to short-range forces are dominant leading to important compensating effects: although the partial wave contributions may be very different, the summations over J (or ℓ) lead to close CC and CS cross sections. In other words the different behavior of the CC and CS calculations is no longer evident after summation over partial waves. Here is the origin for the validity of the CS approximation.[17,18,20]

Similar compensating effects exist also, for low j values, when considering the diagonal elements $\sigma^o(j \rightarrow j, E_{\text{kin}})$, as given by the sum rule [Eq. (3)]. Even if the CC and CS inelastic cross sections may be rather different (Tables I and II), the summation over j' gives diagonal elements that only differ by a few percent: they are not sensitive to the different

TABLE II. Inelastic cross sections (i.e., Raman isotropic line coupling cross sections with opposite sign) in Å^2 for a kinetic energy of 265 cm^{-1} and for low j values. The first line corresponds to the CC results and the second one to the CS results.

j	$j'=j-2$	CS/CC	$j'=j-1$	CS/CC	$j'=j+1$	CS/CC	$j'=j+2$	CS/CC
0					22.63		15.32	
					32.17	1.42	11.29	0.74
1			7.6		18.95		12.29	
			10.83	1.42	20.71	1.09	11.25	0.91
2	3.08		11.57		15.95		10.13	
	2.34	0.76	12.74	1.10	13.37	0.84	13.2	1.30
3	5.46		11.75		13.8		9.42	
	4.97	0.91	10	0.85	9.85	0.71	11.88	1.26
4	5.97		11.24		11.88		9.07	
	7.52	1.26	8.13	0.72	8.57	0.72	8.45	0.93
5	6.35		10.31		9.99		8.12	
	8.2	1.29	7.38	0.71	8.11	0.81	5.98	0.73
6	6.75		9.18		8.86		6.71	
	6.79	1.00	7.27	0.79	8.48	0.96	5.15	0.77

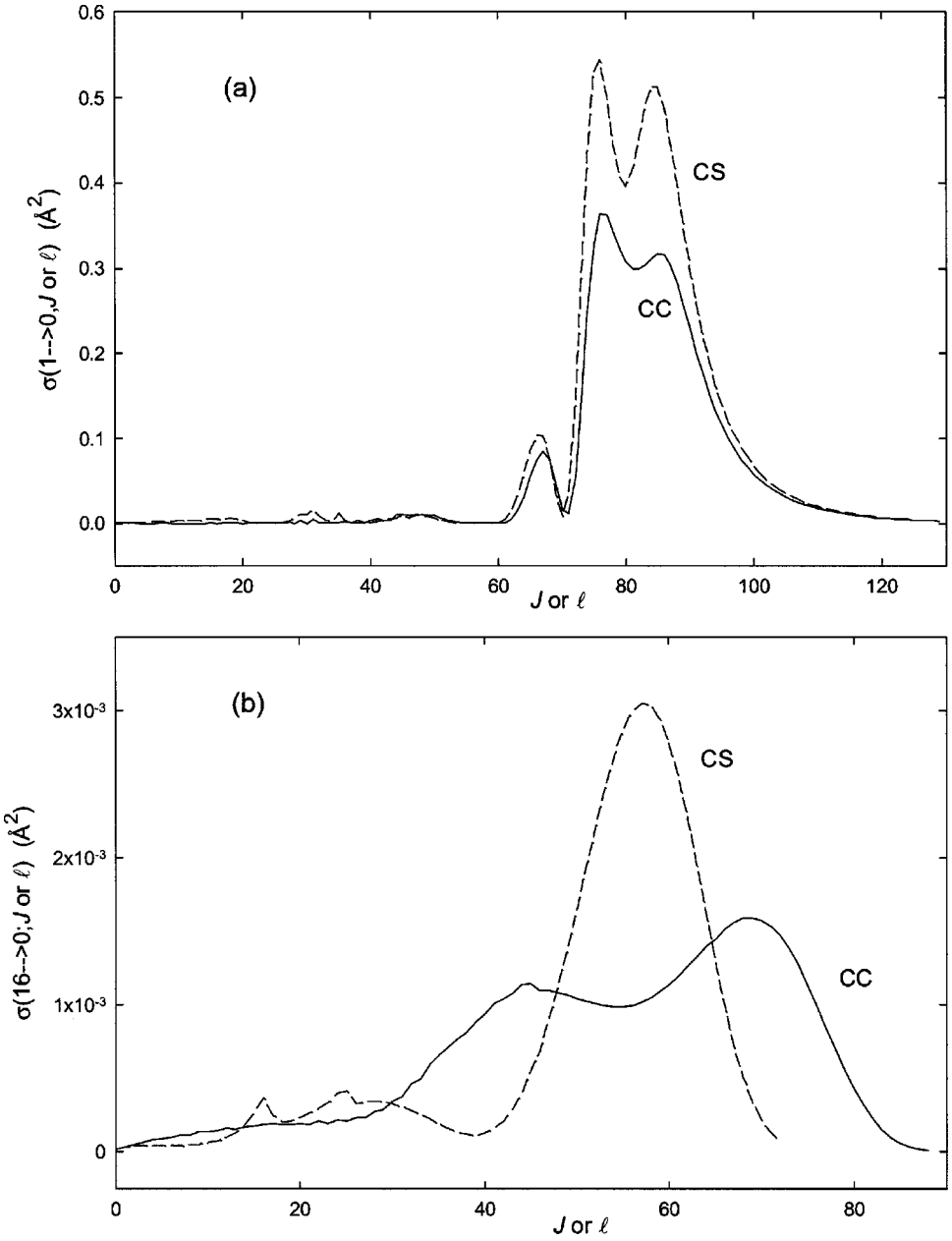

FIG. 1. Comparison of the CC and CS partial cross sections as function of J (or ℓ) at a kinetic energy of 265 cm^{-1} for (a) $\sigma(1\rightarrow 0)$ and (b) $\sigma(16\rightarrow 0)$.

behavior of the CC and CS calculations, except in some cases at low j and low kinetic energies. From that behavior, the limited failing [16% in the worst case: $\sigma^o(3\rightarrow 3,T=87\ K)$] of the CS approach previously noted[8] for the T-dependent diagonal elements may be easily understood. As underlined earlier, similar conclusions were obtained in Refs. 20 and 21 for the CO_2-Ar system.

Consequently, we will consider in the following, cross sections calculated at the CC level, with only a few exceptions corresponding to high j and Δj values. All the T-dependent cross sections are available upon request.

III. ACCURACY OF THE ECS SCALING PROCEDURE FOR INELASTIC CROSS SECTIONS

We are now in a position to check the accuracy of the ECS scaling procedure.

A. ECS scaling formalism

A detailed description of this formalism exists in the literature.[3,4,6] Here we will simply recall the salient points. The ECS inelastic cross sections for initial level j, final level $j'<j$, at temperature T are given, in terms of cross sections to the ground state $L=0$, by

$$\sigma_{\mathrm{ECS}}(j\rightarrow j',T)=(2j'+1)\sum_L (2L+1) \times\begin{pmatrix} j & j' & L \\ 0 & 0 & 0 \end{pmatrix}^2 \sigma(L\rightarrow 0,T)\frac{\Omega_j}{\Omega_L}, \quad (4)$$

where $(\cdots)$ is a $3j$ coefficient and Ω_j is an adiabaticity correction factor which accounts for inelastic energy changes and is usually defined in terms of a collision duration $\overline{\tau_c}$. Note that upward cross sections $j'>j$ are obtained from de-

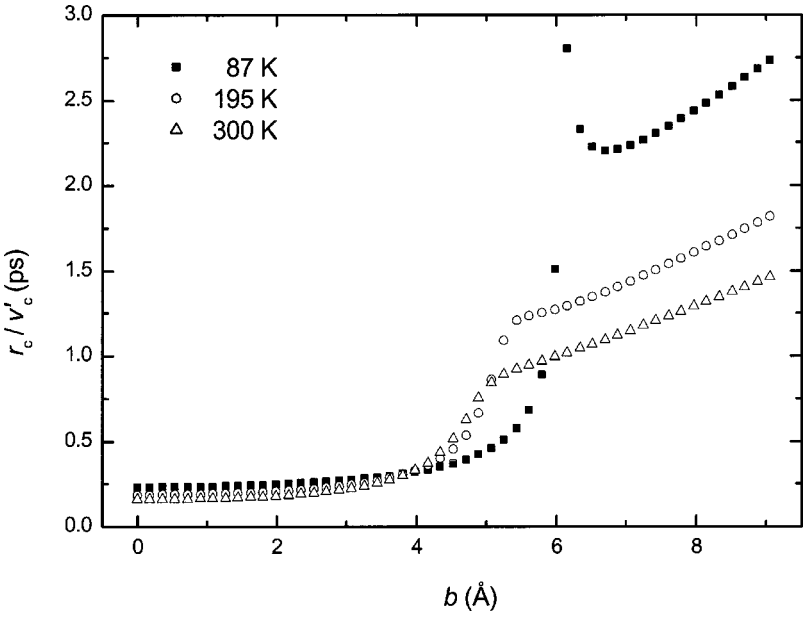

FIG. 2. Duration of collision r_c/v'_c, at $E_{\mathrm{kin}}=(4/\pi)k_BT$ estimated from the trajectory model of Ref. 18.

tailed balance.[7,17] Therefore in the following, the analysis will be restricted to downward cross sections.

B. Various models for adiabaticity factors

In their founding paper, DePristo *et al.*[3] (DP) have introduced the following expression for Ω_j:

$$\Omega_j^{\mathrm{DP}}=[1+\tfrac{1}{24}(\omega_{j,j-1}\overline{\tau_c})^2]^{-2}, \tag{5}$$

where $\omega_{j,j-1}$ is the frequency spacing between adjacent levels and $\overline{\tau_c}$ the critical value of the collision duration. As it was shown that Eq. (5) may lead in some circumstances to unphysical behavior of the ECS formalism, Bonamy *et al.*[22,23] (*B*) have proposed this alternative expression:

$$\Omega_j^{B}=[1+\tfrac{1}{12}(\omega_{j,j-1}\overline{\tau_c})^2]^{-1}. \tag{6}$$

We have also considered for Ω_j an exponential model as proposed by Strekalov.[24]

The appearance in all these models of an effective duration of collision $\overline{\tau_c}$ is an important feature of the scaling relationships. Recall that Eq. (4) has been obtained through a double summation:[3] one over J or ℓ (i.e., over the impact parameter b in a semiclassical frame) and the other over the kinetic energy. In the semiclassical picture, the duration of collision τ_c depends on b and E_{kin}. Therefore an effective duration $\overline{\tau_c}$ appearing in a ''mean'' adiabaticity factor will be physically meaningful and thus only well defined if the major part of the efficient rotational inelastic processes corresponds to collisions of quite similar durations.

C. Results

The input data, $\sigma(L\rightarrow 0,T)$, have been obtained from CC calculations reported in the previous section and are given in Table III. Then, ECS cross sections $\sigma_{\mathrm{ECS}}(j\rightarrow j'<j)$ were computed according to Eq. (4) for three temperatures, $T=300$, 195, and 87 K, and for a number of $\overline{\tau_c}$ values and they were compared with CC results. Note that $\overline{\tau_c}$ will be expressed in the following as $\overline{\tau_c}=\ell_c/\overline{v}$, where $\overline{v}$ is the mean relative velocity and ℓ_c is the scaling length. Since the basic rates $\sigma(L\rightarrow 0,T)$ were calculated up to $L=30$ we have restricted the j values to $2\leqslant j\leqslant 15$. Consequently the sum in Eq. (4) which must be taken over $|j-j'|$ to $|j+j'|$ could be performed without extrapolation of the basic rates. In other words, it remains two adjustable parameters in the model: the adiabaticity factor given by different functional forms and the critical duration of collision $\overline{\tau_c}$.

The accuracy of the ECS scaling has been quantified by considering a mean relative error defined as

$$\langle\varepsilon\rangle=\frac{1}{N}\sum_{jj'}|\sigma_{\mathrm{ECS}}(j\rightarrow j',T)-\sigma_{\mathrm{CC}}(j\rightarrow j',T)|/\sigma_{\mathrm{CC}}(j\rightarrow j',T), \tag{7}$$

TABLE III. Basic CC rate constants $\sigma(L\rightarrow 0)$ in 10^{-3} cm^{-1} atm^{-1}.

L	$\sigma(L\rightarrow 0,T=87\ \mathrm{K})$	$\sigma(L\rightarrow 0,T=195\ \mathrm{K})$	$\sigma(L\rightarrow 0,T=300\ \mathrm{K})$
1	15.8415	8.0582	5.6246
2	8.7133	4.0263	2.6959
3	5.4860	2.3027	1.3934
4	3.0902	1.1665	0.7259
5	4.3130	1.5747	0.9096
6	1.1761	0.4473	0.2759
7	2.3452	0.9757	0.6011
8	0.9969	0.3639	0.2098
9	0.8510	0.4444	0.3128
10	0.8164	0.3328	0.1967
11	0.4789	0.2067	0.1377
12	0.4867	0.2268	0.1515
13	0.3896	0.1489	0.0934
14	0.3228	0.1373	0.0946
15	0.2827	0.1144	0.0719
16	0.2150	0.0852	0.0538
17	0.1677	0.0826	0.0546
18	0.1997	0.0752	0.0455
19	0.0862	0.0613	0.0400
20	0.2500	0.0841	0.0429
21	0.7740	0.1109	0.0440
22	0.0604	0.0178	0.0147

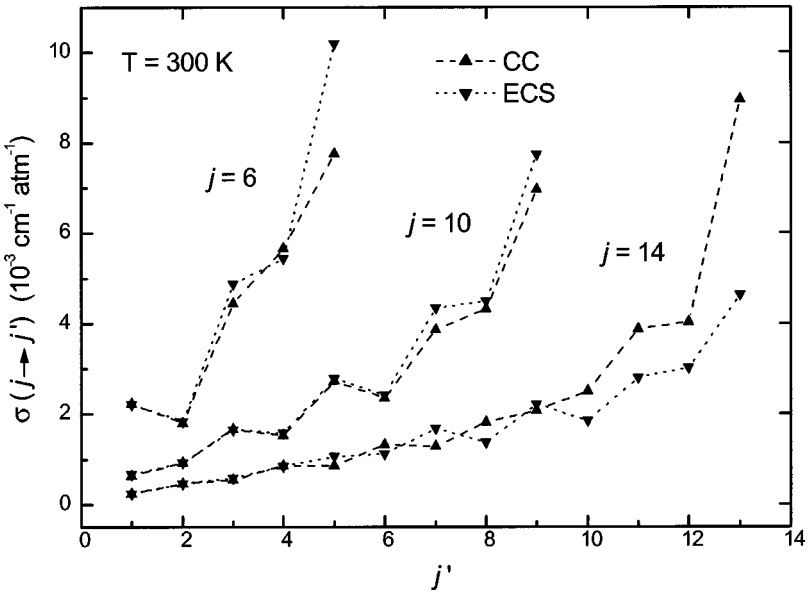

FIG. 3. Comparison of some CC and ECS rate constants $\sigma(j\rightarrow j';T=300\ \mathrm{K})$ for $j=6$, $j=10$, and $j=14$.

where N is the number of cross sections considered and $\langle\varepsilon\rangle$ has been calculated for the various functional forms of the adiabaticity factors and for a grid of $\overline{\tau_c}$ values.

Fits of rather similar quality can be obtained with either the DP or B expressions of Ω_j whereas the model of Strekalov leads to strong disagreement between CS and CC cross sections for any value of $\overline{\tau_c}$. Therefore in the following we shall only discuss calculations made with the Bonamy factor [Eq. (6)].

1. Optimization of $\overline{\tau_c}$

The fit of the ECS scaling [minimization of Eq. (7)] was first done by considering simultaneously the three temperatures. A scaling length around 3 Å allows reproducing the CC results with a mean relative error of about 13%. However, it appears that the value of $\overline{\tau_c}$ that best describes one subset of cross sections for a given temperature is not optimal for another temperature. ECS predictions may therefore be significantly improved while keeping its high level of simplicity just by introducing a scaling length depending on the temperature T so that $\overline{\tau_c}$ increases as T decreases. Note that the optimized value $\overline{\tau_c}(T)$ correlates rather well with the mean duration of collisions calculated for low impact parameters (cf. Fig. 2): $\overline{\tau_c}(T)\approx 2.665\,\langle r_c/v_c'\rangle$ where $\langle r_c/v_c'\rangle$ is the average value of the duration of collisions for $0<b<4$ Å within the parabolic trajectory model (the factor 2.665 represents, in some way, the range of the intermolecular forces). This result is not too surprising since it has been shown earlier that most of the inelastic cross sections used in the fits are governed by collisions with small impact parameters, with the exception of low j and low Δj terms.

As expected from the previous work of Green *et al.*,[6] this test of the ECS scaling seems to be rather positive with average relative errors ranging from 10% to 15%. However, as will be shown in the next section, one must be somewhat cautious in drawing conclusions based on a too global analysis.

2. Weakness of the ECS scaling

Some optimized ECS results are compared with CC data in Fig. 3 for the initial levels $j=6$, 10, 14. ECS predictions are in excellent agreement with CC references with a noticeable exception, the $\Delta j=1$ cross sections, which are reasonably reproduced only around $j=10$. For lower j values, the ECS predictions overestimate these rates and underestimate them at higher j. We have therefore investigated the origin of this quite surprising failing. First, note that $\sigma(1\rightarrow 0,T)$ is the major component to the sum over L in Eq. (4) (its influence vanishes for $\Delta j>1$ cross sections thanks to the $3j$ coefficient). Then remember that $\sigma(1\rightarrow 0,T)$ and more generally $\sigma(j\rightarrow j'=j-1,T)$ for low j values involve important contributions from inelastic cross sections with large angular momentum (or classical impact parameter b). It has been shown in Fig. 2 that the duration of that type of collision strongly varies with b and differs significantly from the duration of short-range collisions. Consequently, in that situation, the concept of a mean adiabaticity factor losses its physical meaning. Moreover it has also been demonstrated that in these cases the CS approximation is less accurate than expected and that CC calculations are required. However, the introduction by DePristo *et al.*[3] of an adiabaticity factor based on a classical trajectory can only be understood within the CS limit (how to introduce in the CC formalism adiabaticity corrections based on a classical description of translation for $\Delta\ell\neq 0$ contributions?), so part of this failing should also be related to the CS approximation.

The weakness of the ECS scaling has a severe consequence if one tries now to calculate the diagonal elements through a sum rule similar to Eq. (3),

$$\sigma^{o}_{\mathrm{ECS}}(j\rightarrow j,T)\approx -\sum_{j'\neq j}\sigma^{o}_{\mathrm{ECS}}(j\rightarrow j',T). \tag{8}$$

First of all, it must be emphasized that, contrary to Eq. (3) which is exact both for the CC and CS schemes, Eq. (8) is only approximate since, as is underlined in Ref. 3, the ECS

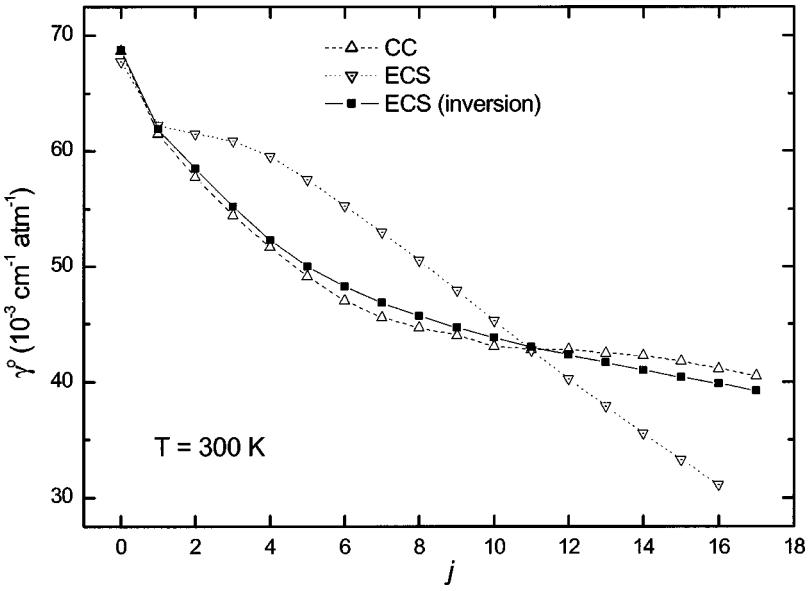

FIG. 4. Comparison between CC (△) and ECS broadening coefficients (in 10^{-3} cm^{-1} atm^{-1}) for $T=300$ K. (▽) ECS results from basic CC cross sections through Eqs. (4), (6), and (8) and using $\ell_c=3.5$ Å. (△): Results of the ECS inversion procedure: the basic rates are modeled by Eq. (9) and the optimized parameters (note that $\ell_c=8.8$ Å) are given in Table V.

energetic corrections do not guarantee the unitarity of the S matrix. Therefore the rather disappointing predictions of Eq. (8), as shown in Fig. 4, are easily understood if one remembers that the two major components σ^o_{ECS} $(j\rightarrow j\pm 1,T)$ to the diagonal elements are poor predictions of the true cross sections. The overestimation of the broadening cross sections observed at low j (and underestimation at high j) may be interpreted from the results of Fig. 3.

IV. ACCURACY OF THE USUAL INVERSION PROCEDURE

We are now in a position to shed more light on the usual ECS *inversion* procedure[4,25,26] which is mainly used to model rotational energy transfer as well as the various relaxation matrices involved in IR and Raman spectroscopy, where line-mixing effects are important. Let us briefly recall that inversion procedure.

(i) Equation (8) is assumed to be sufficiently accurate to model the diagonal elements which are related to the line broadenings and can be easily measured.

(ii) The basic rates are modeled through a reasonable fitting law, generally a hybrid exponential-power (EP) law involving some adjustable parameters,[2,4] such as

$$\sigma(L\rightarrow 0,T)=\frac{A(T)}{[L(L+1)]^{\alpha}}\exp(-\beta E_L/k_BT). \tag{9}$$

(iii) These parameters and the critical duration of collisions $\overline{\tau_c}$ (which enters in the adiabaticity factor) are thus determined by inversion of the experimental data through Eqs. (8) and (4).

We have followed exactly this procedure, using as input data the CC diagonal elements (recall that these theoretical results have been shown to be very accurate[8,27]). As shown in Fig. 4, the fit of ECS broadening coefficients is excellent so it could be concluded that the ECS inversion procedure accurately predicts linewidths. However, here too, one must be cautious since the inversion procedure does not provide a realistic representation of *all* the fundamental cross sections $\sigma(L\rightarrow 0,T)$. Indeed, as it appears from Fig. 5, the agreement between "exact" and inverted individual scaling rates is rather satisfactorily at low L values $(L\leqslant 15)$. Of course the propensity to transitions to odd L values observed for the CC calculations cannot be reproduced, but the average rates are well predicted. Note that the agreement is similar to inverted rates previously obtained by DePristo and Rabitz[28] through a rather different scaling theoretic deconvolution of pressure broadened linewidths as it appears from Table IV. At higher L, inverted basic rates, as given by Eqs. (8) and (9), strongly differ from the "exact" ones and therefore must be considered as effective rates. Moreover the duration of collisions as given by the inversion procedure (Table V) $\overline{\tau_c}\sim 1.42$ ps is more than twice that previously determined (cf. Sec. III, $\overline{\tau_c}\sim 0.56$ ps for $\ell_c=3.5$ Å). Note that the optimized parameters obtained here (Table V) are practically identical to those derived by Belikov and Smith[10] from experimental IR linewidths. This divergence of the basic rates at high L values together with the necessity of a too high $\overline{\tau_c}$ value may be easily understood from the above analysis of the ECS scaling of the inelastic cross sections: for instance at high j (cf. Fig. 4), the inversion procedure compensates the underestimation of the linewidths as given by the ECS scaling law [Eq. (8)], by increasing the high L contributions through an increase of the adjustable $\sigma^o(L\rightarrow 0,T)$ basic rates together with a too high value of the duration of collision.

These results are not so bad: the ECS inversion procedure provides fundamental rates $\sigma^o(L\rightarrow 0,T)$ in reasonable agreement with the CC ones (to within about 20%) up to $L=15$, i.e., over a range where the basic rates themselves vary by two orders of magnitude. They corroborate similar results obtained with CO_2–argon.[26] However, for $L>15$, the inverted rates diverge. Since the inversion method also leads to an overestimation of the effective duration of collisions, its ability to reproduce any experiment sensitive to the moderate and high j part of the relaxation matrix may be questionable, since it is known that basic rates for high L values are needed for convergence in that part of the matrix.[26]

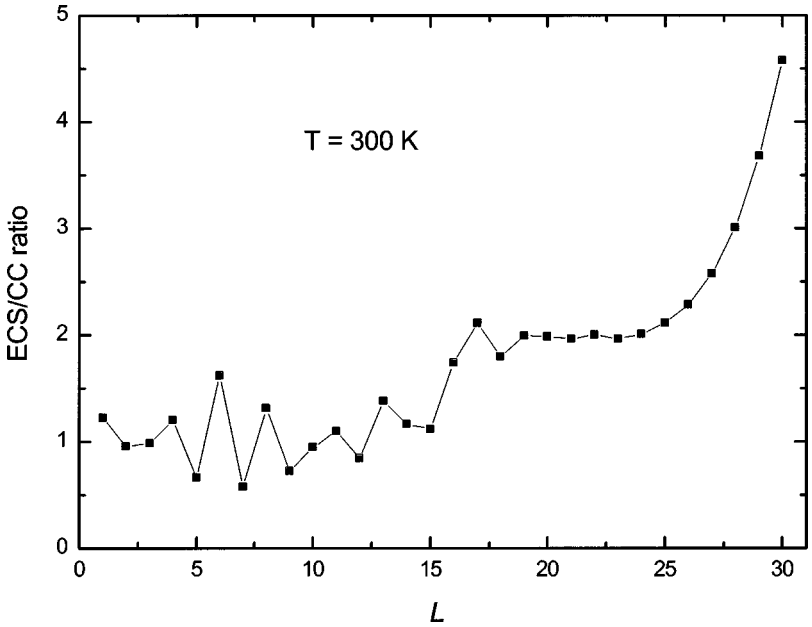

FIG. 5. Ratio of ECS inverted basic rates $\sigma(L\rightarrow 0, T=300\ \mathrm{K})$ to the corresponding CC basic rates as a function of L.

V. COMPARISON WITH EXPERIMENT: CLOSE COUPLING CALCULATIONS OF STIMULATED RAMAN *Q* BRANCH OF CO IN ARGON

As is now well established, line shapes provide information about rotational relaxation matrices for overlapping lines where collisions can transfer intensity among different spectral lines. Rotational lines in Q branches are closely spaced so line coupling is very important even at moderate perturber densities, leading to a spectral line shape very sensitive to the off-diagonal elements of the relaxation matrix. Moreover, isotropic Raman Q branch is by far the most interesting test since in that case, when vibrational dependence can be ignored, the relaxation matrix coupling $Q(j)$ to $Q(j')$ is just the inelastic state-to-state rate $\sigma(j\rightarrow j',T)$ with opposite sign. Therefore the fundamental isotropic Raman Q branch of CO has been recorded using stimulated Raman spectroscopy for mixtures with argon in the temperature range 87–300 K and the spectra have been compared with theoretical band shapes based on CC relaxation matrix presented in Sec. II.

TABLE IV. Comparison of calculated CC basis rate constants $\sigma(0\rightarrow L,T)$ in 10^{-10} cm^3 molecule^{-1} s^{-1} at $T=300$ K (this work) with those derived by DePristo *et al.* (Ref. 28) and Belikov and Smith (Ref. 10).

L	DePristo *et al.*[a]	Belikov and Smith[b]	This work
1	0.99	1.57	1.284
2	0.91	0.94	0.99
3	0.77	0.67	0.678
4	0.6	0.506	0.425
5	0.44	0.392	0.588
6	0.31	0.306	0.189
7	0.20	0.24	0.419
8	0.13	0.186	0.1423

[a]Reference 28.
[b]Reference 10.

A. Experiment

Measurements were made with the stimulated Raman loss spectrometer in Madrid. The experimental setup has already been described in detail elsewhere.[29,30] The specific details of this experiment are similar to those described in a previous work on line mixing effects in CO–He mixtures.[7] In the present case, the proportion of CO in the mixture was increased up to 2% in order to improve the signal-to-noise ratio. Measurements were made at room and low temperatures (300, 195, and 87 K).

For the 195 K measurements, a 2-cm-diam and 80-cm-long cell with Brewster angle windows (also used at 300 K) was packed in dry ice. For the 87 K measurements, another Brewster angle windows cell having the same dimensions with a double jacket was used. The inner jacket was filled with liquid Ar. The outer jacket was evacuated and covered with mylar film in order to provide the necessary thermal isolation. In both cases, a portion of about 8 cm at each end of the cell was outside the cooling bath but, as the Raman signal is mostly generated in the Rayleigh range of the focused lasers (a few mm in the present case), no significant contribution to the spectrum was expected from molecules in the warmer ends of the cell. Nevertheless this assumption was checked by recording low pressure spectra of pure CO and verifying that intensities of the rotational lines in the Q

TABLE V. Fitted parameters from the ECS inversion procedure [see Eqs. (4), (6), and (9)] at $T=300$ K.

Parameters	Present work	Belikov *et al.*[a]
A (10^{-3} cm^{-1} atm^{-1})	12.704	13.2
β	0.0156	0.0156
α	0.895	0.895
ℓ_c (Å)	8.8	8.8
$\overline{\tau_c}$ (10^{-12} s)	1.417	1.417

[a]Reference 10.

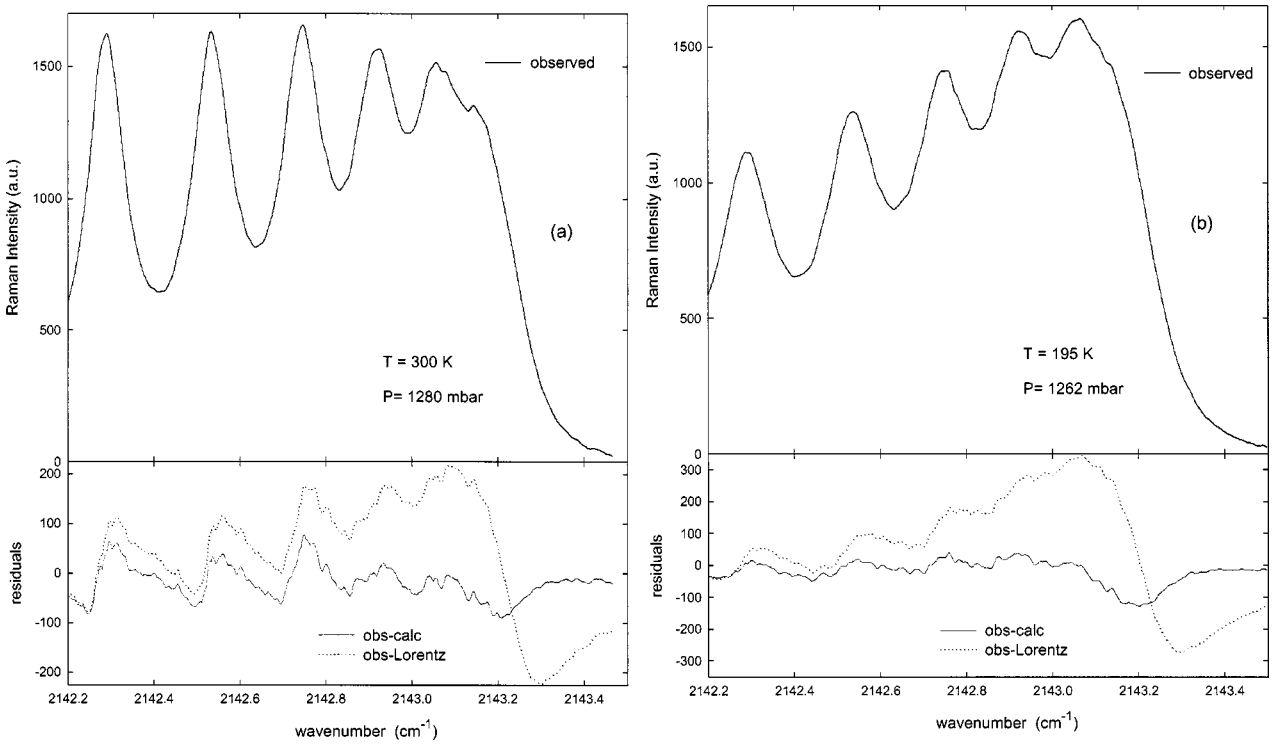

FIG. 6. Experimental spectra for $T=300$ K (a) and 195 K (b) at the higher pressures used. The bottom box allows comparing the CC calculations (full relaxation matrix) or the sum of Lorentzian lines (only diagonal elements of the relaxation matrix are considered) to the experimental spectra.

branch were compatible with a Boltzmann distribution at the expected temperatures.

Except at 87 K, the spectra were recorded at nominal pressures of 50, 250, 500, 750, 1000, and 1250 mbar. For 87 K the maximum pressure was 900 mbar. As described in Ref. 7, particular attention was paid to the linearity of the detection system and to the stability of the baseline.

In the 87 K series a strong deviation of the trajectory of the lasers traveling through the cell was observed for the higher pressure measurements. Actually, for 750 and 900 mbar, if the cell was aligned at room temperature, an angular realignment was necessary after cooling it, in order to get the laser beams out of the cell on the other end. The spatial profile of the lasers after passing the cell was satisfactorily clean even in the far field (several meters away), so we estimated the formation of droplets as negligible. As the shape of the cell was that of a prism with antiparallel Brewster angle windows, we concluded that a huge change in the refractive index of the medium (mainly Ar) took place when cooling; this change should be much stronger than expected from the temperature dependence of the refractive index of a gas. Since the proportion of aggregates is expected to be low (about 2.5% of Ar dimers[31]), we do not have at present any reasonable explanation for this phenomenon that may be related to the lack of agreement between calculation and experiment for the low temperature, high pressure data.

B. Comparison between theoretical and experimental profiles

The fundamental theory describing the line shape in terms of collisions theory S matrix is well known and was described, for instance, in our previous work devoted to the CO–He system; this theory will not be reviewed in this paper (see Sec. II A and Sec. IV of Ref. 7).

Figures 6 and 7 present a comparison of experimental Q-branch spectra with the theoretical profiles obtained from the CC relaxation matrices. The importance of line coupling is emphasized by showing predictions of sum of Lorentz profiles. At 300 and 195 K, for argon pressures lower than 1 bar the observed spectra are much better described by taking into account line-mixing effects than using a simple sum of Lorentz line profiles (no coupling). Agreement is seen to be satisfactory with the exception of the lowest temperature where the theory fails at reproducing the observed spectra for the highest perturber densities [Fig. 7(b)]. At low density, owing to the rotational dependence of the line spacing, line-mixing effects are negligible (with the exception of $j=0$ and $j=1$) so the good agreement between theory and experiment clearly indicates that the diagonal elements $\sigma^o(j\rightarrow j,T=87\ \mathrm{K})$ are accurately predicted from the potential of Ref. 9, corroborating a previous analysis.[8,27] As outlined earlier, we have no clear explanation for the discrepancies observed at higher densities. Of course the accuracy of the IPS may be questioned: Scheele *et al.*,[32] for instance, have criticized the deeper part of the TC potential from an analysis of the spectrum of the Ar–CO complex. However, a very similar IPS has been recently published[33] which leads to close results with the TC IPS for both the energy levels of the complex and the linewidths.[27] Similarly, the validity of the impact approximation may be questionable near the vapor pressure curve. Finally, CO–Ar complexes should bind about 4% of CO molecules,[31] which seems to be too low to provide any

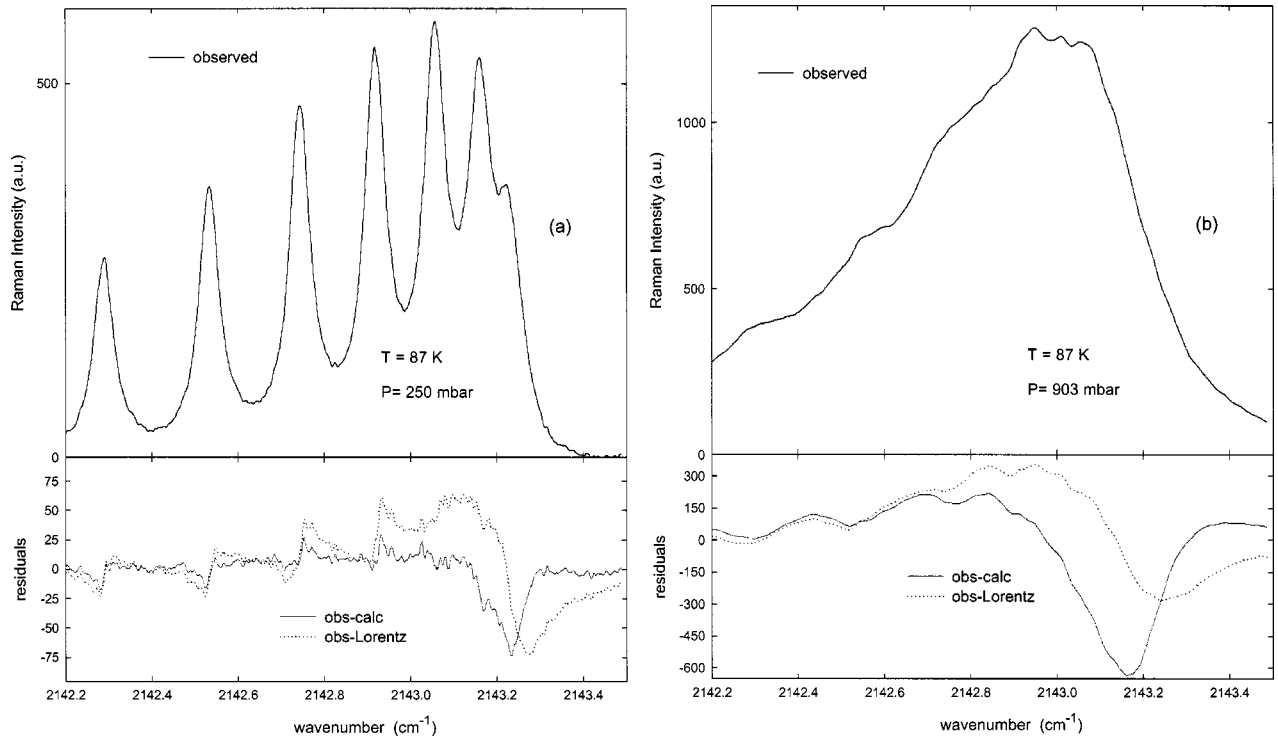

FIG. 7. Experimental spectra for $T=87$ K at 250 mbar (a) and 903 mbar (b). The observed minus calculated residuals are shown at the bottom of each layer which allow us to compare CC results and the sum of Lorentz lines.

detectable signature. It would now be very desirable to perform similar measurements at much higher pressures for high temperatures and also to carefully investigate at low temperature the highest densities consistent with the gas state.

VI. COMPARISON WITH EXPERIMENT: ROTATIONAL RELAXATION TIME MEASURED IN FREE JETS

Rotational state-to-state rate coefficients may also be tested from the measured evolution of the nonequilibrium rotational energy measured in shock waves or free supersonic jets. These data may be compared with computational results based on kinetic equations. Belikov and Smith[10] have studied the rotational relaxation of CO in CO–Ar free jets in the temperature range from 7 to 150 K. As a preliminary test we have calculated the rotational relaxation time τ_R, related to the CC rates by

$$\overline{v}\sigma_R(T)=(n_b\tau_R)^{-1}=\sum_{j'}\sum_{j>j'}\sigma(j\to j';T)N_j^*\frac{(E_j-E_{j'})^2}{\langle E^2\rangle-\langle E\rangle^2} \tag{10}$$

where N_j^* is the equilibrium population of the jth rotational level and $\langle E^n\rangle=\Sigma_j N_j^* E_j^n$ are the rotational energy moments. The (effective) cross sections σ_R are compared to the values derived from measurements[10] in Fig. 8. Our results exceed the experimental values by about 50%. It should be noted however that the present theoretical results are in as good agreement as the best empirical model based on fitting rates considered by Belikov and Smith[10] (SPEG model). Note also that the present work invalidates the explanation of this discrepancy on σ_R by the possible importance of reorientation cross sections which could influence the inversion of IR pressure broadening cross sections since that procedure is not necessary here because the whole isotropic relaxation matrix has been ''exactly'' calculated.

In another experiment, Kruss[34] used the infrared absorption in crossed jets in order to determine the ratio $\sigma(1\to 0)/\sigma_d$ for CO–Ar at room temperature with $\sigma_d=\Sigma_{j'\geqslant 2}\sigma(0\to j')$. He assumed that $\Sigma_{j'\geqslant 2}\sigma(0\to j')/\Sigma_{j'\geqslant 2}\sigma(1\to j')\approx 1$, whereas we find 1.07 from our calculations. Then Kruss obtained $\sigma(1\to 0)/\sigma_d\approx 0.2$ whereas our result is 0.3, which is not so bad given the nature of the experiment.

Here, too, we have no clear explanation for the overestimation of the rotational relaxation cross sections at very low temperatures. Since state-to-state cross sections for very low kinetic energies strongly depend on the long-range part of the potential, the accuracy of the potential may be invoked once more. However, the interpretation of this type of experiment is far from being obvious[35] and a more detailed study will be necessary for any definitive conclusion. The benchmark close-coupling calculations presented here may be used for the analysis of the experimental results of Ref. 10 at a more elementary level, like the evolution of the rotational level populations as a function of the distance from the nozzle, etc.

VII. CONCLUSION

We have carried out benchmark close-coupling calculations of the whole relaxation matrix of CO in argon in a rather wide range of temperatures. Extending a previous work by Green *et al.*,[6] we have shown that provided accurate

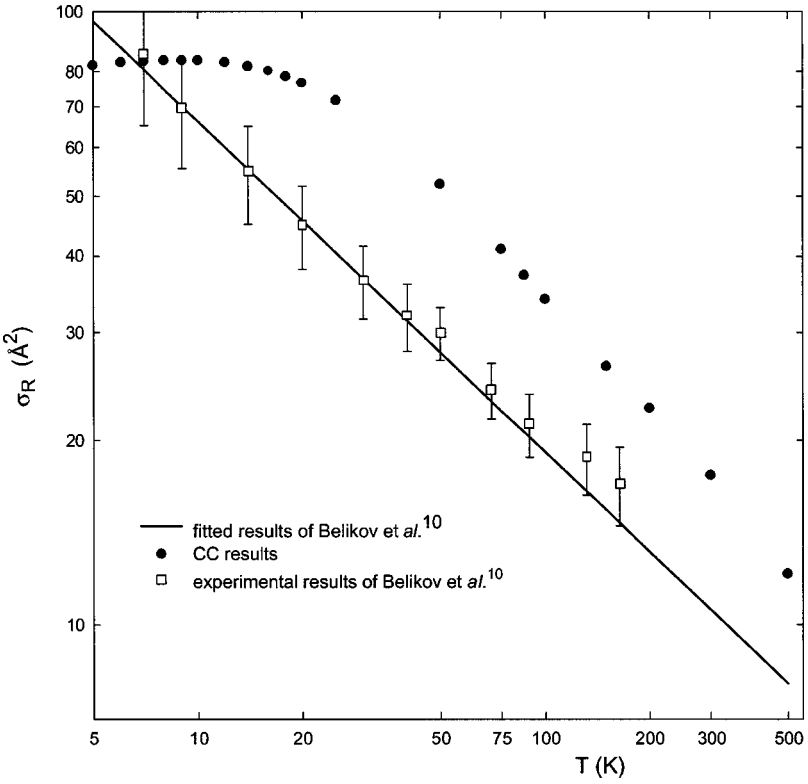

FIG. 8. Comparison of the cross sections for the relaxation of the mean rotational energy as derived from CC rates with the experimental values of Belikov and Smith (Ref. 10). The straight line corresponds to one of the experimental law given in Ref. 10 [Eq. (13)]. The points correspond to the data of Fig. 5 in Ref. 10.

values are available for the basic rate constants $\sigma(L \rightarrow 0,T)$, the ECS scaling procedure may be used to generate the whole relaxation matrix, at least for most of the populated levels with an average error of about 15%. However this conclusion must be tempered by the important discrepancies which have been observed between CC and ECS predictions for the most important contributions $(j \rightarrow j' = j \pm 1)$. Then we have demonstrated that an inversion procedure based on the ECS scaling law provides basic rates in reasonable agreement with CC data. However, it should be noted that the method leads to unrealistic values for the high L basic rates, due to the fact that the ECS cross sections cannot intrinsically verify the sum rule.

Finally, some exploratory calculations have been done for the isotropic Raman profiles of CO in Ar at moderate temperatures and densities and for rotational relaxation cross sections at low temperatures. The level of agreement is, in some cases, disappointing. However it seems reasonable to claim that a more stringent test of the potential now requires new experimental measurements of the Raman profile at much higher densities together with a more detailed analysis of the measurements in free jets. We estimate that the CC results reported here will be valuable for such future studies.

ACKNOWLEDGMENTS

We gratefully acknowledge fruitful discussions with Dr. A. Vigasin (Moscow) on the possible influence of CO–Ar complexes. D.B. and J.L.D. acknowledge financial support from Spanish DGI under Project No. REN2002-01618.

[1] S. P. Phipps, T. C. Smith, G. D. Hager, M. C. Heaven, J. K. McIver, and W. G. Rudolph, J. Chem. Phys. **116**, 9281 (2002).
[2] T. A. Brunner and D. Pritchard, Adv. Chem. Phys. **50**, 589 (1982).
[3] A. E. DePristo, R. Ramaswamy, S. D. Augustin, and H. Rabitz, J. Chem. Phys. **71**, 850 (1979).
[4] G. Millot, J. Chem. Phys. **93**, 8001 (1990).
[5] A. Levy, N. Lacome, and C. Chackerian, Jr., in *Spectroscopy of the Earth Atmosphere and Interstellar Medium* (Academic, New York, 1992), pp. 231–337.
[6] S. Green, D. L. Cochrane, and D. G. Truhlar, J. Chem. Phys. **84**, 3865 (1986).
[7] J. Boissoles, F. Thibault, J. L. Domenech, D. Bermejo, C. Boulet, and J.-M. Hartmann, J. Chem. Phys. **115**, 7420 (2001).
[8] F. Thibault, R. Z. Martinez, J. L. Domenech, D. Bermejo, and J.-P. Bouanich, J. Chem. Phys. **117**, 2523 (2002).
[9] R. R. Tockzylowski and S. M. Cybulski, J. Chem. Phys. **112**, 4604 (2000).
[10] A. E. Belikov and M. A. Smith, J. Chem. Phys. **110**, 8513 (1999).
[11] F. Thibault, R. Le Doucen, J.-P. Bouanich, and C. Boulet, J. Mol. Spectrosc. **171**, 576 (1995).
[12] A. M. Arthurs and A. Dalgarno, Proc. R. Soc. London, Ser. A **256**, 540 (1960).
[13] S. Green, J. Boissoles, and C. Boulet, J. Quant. Spectr. Rad. Transf. **39**, 33 (1988).
[14] R. Goldflam and D. J. Kouri, J. Chem. Phys. **66**, 542 (1977).
[15] D. R. Flower, G. Bourhis, and J.-M. Launay, Comput. Phys. Commun. **131**, 187 (2000).
[16] J. M. Hutson and S. Green, MOLSCAT version 14, Collaborative Computational Project No. 6 of the Science and Engineering Research Council (UK).
[17] F. A. Gianturco, in *Collision Theory for Atoms and Molecules*, edited by F. A. Gianturco, NATO Series Vol. B196 (Plenum, New York, 1989); D. J. Kouri, in *Atom-Molecule Collision Theory (a Guide for Experimentalist)*, edited by R. B. Bernstein (Plenum, New York, 1979).
[18] J.-M. Launay, J. Phys. B **9**, 1823 (1976).
[19] D. Robert and J. Bonamy, J. Phys. (France) **40**, 923 (1979).
[20] C. F. Roche, A. S. Dickinson, and J. M. Hutson, J. Chem. Phys. **111**, 5824 (1999).
[21] F. Thibault, B. Calil, J. Buldyreva, M. Chrysos, J.-M. Hartmann, and J.-P. Bouanich, Phys. Chem. Chem. Phys. **3**, 3924 (2001).
[22] L. Bonamy, J. M. Thuet, J. Bonamy, and D. Robert, J. Chem. Phys. **95**, 3361 (1991).
[23] L. Bonamy and J. V. Buldyreva, Phys. Rev. A **63**, 012715 (2000).
[24] M. L. Strekalov, Mol. Phys. **86**, 39 (1995).

[25] J. Boissoles, F. Thibault, and C. Boulet, J. Quant. Spectrosc. Radiat. Transf. **56**, 835 (1996).
[26] F. Thibault, J. Boissoles, C. Boulet, L. Ozanne, J.-P. Bouanich, C. Roche, and J. M. Hutson, J. Chem. Phys. **109**, 6338 (1998).
[27] A. W. Mantz, F. Thibault, J. L. Cacheiro, B. Fernandez, T. B. Pedersen, H. Koch, A. Valentin, C. Claveau, A. Henry, and D. Hurtmans, J. Mol. Spectrosc. (unpublished).
[28] A. E. DePristo and H. Rabitz, J. Chem. Phys. **68**, 1981 (1978).
[29] A. Owyoung, C. W. Patterson, and R. S. McDowell, Chem. Phys. Lett. **59**, 156 (1978).
[30] J. Santos, P. Cancio, J. L. Rodriguez, and D. Bermejo, Laser Chem. **12**, 53 (1992).
[31] A. Vigasin (private communication).
[32] I. Scheele, R. Lehnig, and M. Havenith, Mol. Phys. **99**, 205 (2001).
[33] T. B. Pedersen, J. L. Cacheiro, B. Fernàndez, and H. Koch, J. Chem. Phys. **117**, 6562 (2002).
[34] E. J. Kruss, J. Phys. Chem. **98**, 3099 (1994).
[35] F. J. Aoiz, L. Banares, V. J. Herrero, B. Martinez-Haya, M. Menendez, P. Quintana, I. Tanarro, and E. Verdasco, J. Phys. Chem. A **105**, 6976 (2001).